Fault Current Limitation Coordination in Electric Power Grid with Superconducting Fault Current Limiters

N. Hayakawa, *Member, IEEE*, Y. Maeno, H. Kojima, *Member, IEEE*

***Abstract*— This paper proposes the concept of "fault current limitation coordination" in a future electric power grid with multiple superconducting fault current limiters (SFCL). Not only the fault current limitation of each SFCL on a transmission line, but also the transient stability of the grid with SFCLs should be taken into account, because the disturbance is brought about in the grid by the sudden appearance and disappearance of a large impedance of SFCL at the fault current limitation and recovery after the fault clearance, respectively. In this paper, both of the fault current limitation of SFCLs and the internal phase angle oscillation of generators were calculated by PSCAD/EMTDC to evaluate the operational feasibility or coordination of SFCLs in a 275/77 kV transmission system model.**

***Index Terms*— superconducting fault current limiter, electric power grid, fault current limitation, transient stability, coordination**

I. Introduction

SUPERCONDUCTING fault current limiters (SFCL) are expected to keep zero impedance in the steady state of a power system and generate high impedance at the fault occurrence in the power system, irrespective of the SFCL types (resistive, shielded iron core, saturated iron core, etc.) [1]-[3]. The generated impedance of SFCL limits the fault current larger than the critical current of SFCL and is expected to return to zero after the fault clearance. Thus, the fault current limitation and recovery operation of SFCL brings about a sudden appearance and disappearance of impedance in the power system, both of which may cause a disturbance in the operation of total power system with SFCL, even if the fault current could be effectively limited. Especially, in an electric power grid of European countries, etc., multiple SFCLs will be introduced and their operational feasibility or coordination between SFCLs should be taken into account.

From the above background, this paper proposes the concept of "fault current limitation coordination" in a future electric power grid with multiple SFCLs. Fig. 1 shows the conceptual diagram of "fault current limitation coordination", which can be an analogy of "insulation coordination" of arresters in high voltage issues. Fault current limitation coordination means the mutual relationship between prospective fault current (I_{pro}) of a transmission line in a grid, quench current (I_{quench}) of protected equipment such as HTS cables, limited current (I_{1st}) after fault and limitation, critical current (I_c) of SFCL, and operating current (I_{op}) before fault. In this paper, focusing on the ratios of I_c/I_{pro} and I_{op}/I_c, we calculated the fault current limitation and the transient stability of a 275/77 kV transmission system model with resistive-type SFCLs and discussed the operational coordination of SFCLs.

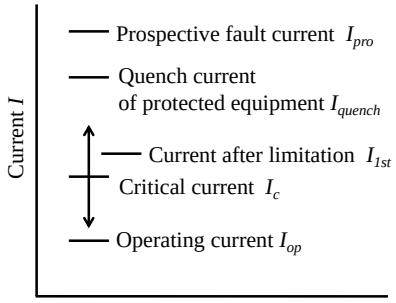

Fig. 1. Conceptual diagram of fault current limitation coordination

II. Models and Simulation Methods

A. Model of HTS tape

In order to quantitatively investigate the "fault current limitation coordination", we used an analytical approach with the modeling of resistive-type SFCL and an electric power grid. SFCL was modelled by a variable resistance as a function of both current *I* and temperature *T*. Fig. 2 shows the *E-I-T* characteristics of the HTS tape in Table 1 as our experimental database [4], where *E* is the electric field strength along the HTS tape length. In the *E-I-T* characteristics in Fig.2, there exist 2 lines with different slopes at each temperature, which corresponds to the flux flow regions E_A and E_B, respectively, as shown in Fig. 3 [5]. Each region in Fig. 3 can be expressed as follows:

Superconductor: $E_{sc} = E_0\{I / I_c(T)\}^n$

Flux flow A: $E_{flux-flow-A}(I,T) = A(T)I^{N_1(T)}$

Flux flow B: $E_{flux-flow-B}(I,T) = B(T)I^{N_2(T)}$

Normal: $E_{normal}(I,T) = C(T)I$

N. Hayakawa, Y. Maeno, and H. Kojima are with the Department of Electrical Engineering, Nagoya University, Nagoya 464-8603, Japan (e-mail: nhayakaw@nuee.nagoya-u.ac.jp, kojima@nuee.nagoya-u.ac.jp)

Table 1. Specifications of HTS tape

HTS layer	YBCO (2 μm)
Stabilizer	Ag (2 μm)
Buffer layer	Alumina/YSZ/IBAD MgO/MgO/LMO
Substrate	Hastelloy (100 μm)
Total thickness	0.1 mm
Width	12 mm
Ic @ 77K, self field	220 A (0.3 μV/cm)
n value@Ic	36.5

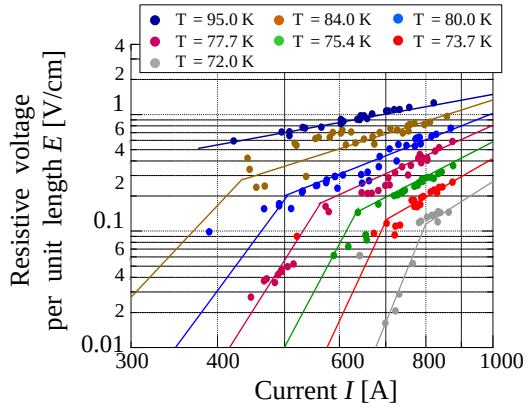

Fig. 2. *E-I-T* characteristics of HTS tape (experimental database) [4]

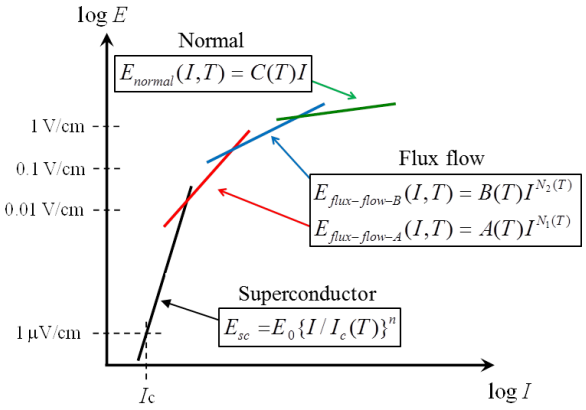

Fig.3. *E-I-T* characteristics of HTS tape (schematic illustration) [5]

E_0 is the reference field (= 0.3 μV/cm) and n is the n value (= 36.5) for the HTS tape in Table 1. The temperature-dependent coefficients $A(T)$, $B(T)$, $C(T)$, $N_1(T)$, $N_2(T)$ are obtained by fitting the experimental database in Fig. 2.

Fig. 4 shows $I_c(T)$ of the HTS tape in Table 1 [6]. The vertical value is normalized by the critical current at 77 K and I_c at 95 K is 0 A. The temperature rise of the HTS tape was calculated by solving the following heat conduction equation:

$$C_v(T)\frac{dT}{dt} = R_{sc}(t)I(t)^2 - q(\Delta T)P_{sc}$$

$C_v(T)$ and $R_{sc}(t)$ are the thermal capacity and resistance of HTS tape, $q(\Delta T)$ is the heat flux to LN_2 and P_{sc} is the cooling area. Fig. 5 shows $C_v(T)$ per unit length and Fig. 6 shows $q(\Delta T)$ for different temperatures.

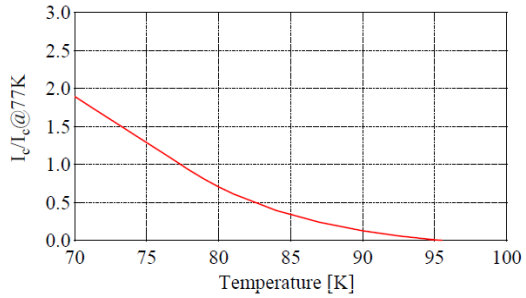

Fig. 4. Temperature dependence of critical current

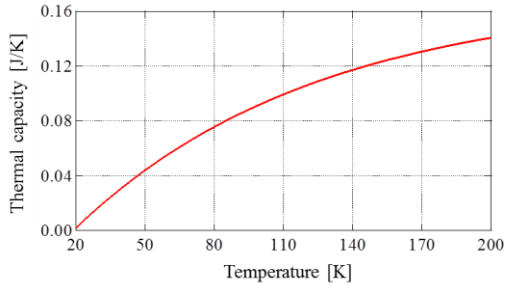

Fig. 5. Thermal capacity of HTS tape

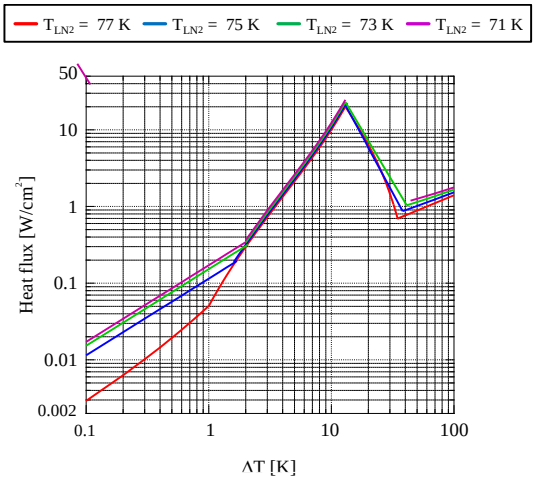

Fig. 6. Heat flux to LN_2 for different temperatures

B. *Model of power system*

Fig. 7 shows the model of power system in this paper. The model system simulates an electric power grid of 275/77 kV transmission system with 2 generators, 6 transformers, 7 lines and the total load of 185 MW [7]. Table 2 shows the parameters of generators, transmission lines and transformers in Fig. 7, where SFCL1 on Line5 and SFCL2 on Line6 are introduced, respectively, and three-phase ground fault is assumed to occur at the bus of sub-station SS5 for 5 cycles. Each SFCL is designed to have the length depending on the rated voltage and current of the transmission line at the introduction point.

Supposing the introduction of multiple SFCLs and the fault points in different lines in Fig. 7, we calculated the fault current limitation by SFCLs and the internal phase angle oscillation of generators as the transient stability for different combinations of I_c/I_{pro} between 0.1 and 0.6 for each SFCL by changing I_c, i.e. the number of paralleled HTS tapes. PSCAD/EMTDC as one of the electromagnetic transient simulation tools was used for such a coupled analysis of short-term and long-term simulation.

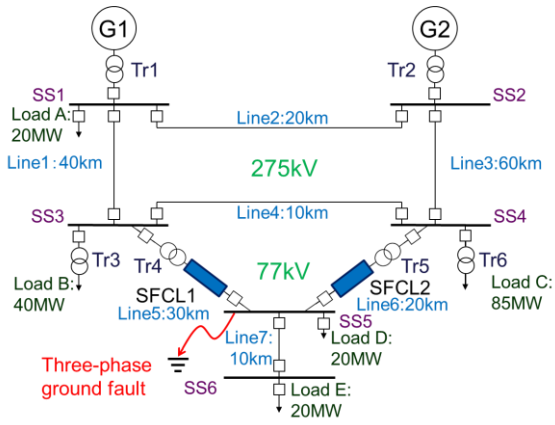

Fig. 7. Model system with SFCLs

Table 2. Parameters of generators, transmission lines and transformers

Generators	G1	G2
Rated power	100 MW	200 MW
Rated voltage	22 kV	22 kV
Xd, Xd', Xd''	1.569, 0.324, 0.249 pu	1.651, 0.232, 0..171 pu
Xq, Xq', Xq''	1.548, 0.324, 0.248 pu	1.590, 0.380, 0.171 pu
Xl	0.204 pu	0.102 pu
Td0', Td0'', Tq0', Tq0''	5.14, 0.0437, 0.50, 0.070 s	5.90, 0.033, 0.535, 0.078 s

Transmission lines	Line1 - Line4	Line6 - Line8
Resistance	0.03 ohm/km	0.0124 ohm/km
Inductance	0.96 mH/km	0.3 mH/km
Capacitance	0.011 microF/km	0.37 microF/km

Transformers	Tr1 - Tr6
Capacity	50 MVA
Leakage impedance	5%

III. Simulation Results and Discussion

A. *Current limitation and transient stability*

Fig. 8 shows (a) current waveform of Line5 and (b) internal phase angle waveform of G1, respectively, for different combinations of I_c/I_{pro} of SFCL1 and SFCL2 in Fig. 7. In the case of I_c/I_{pro} =0.1 for both SFCLs, the fault current of Line5 at the first cycle after fault was effectively limited to 27 % of that without both SFCLs. On the other hand, in the case of $(I_c/I_{pro})_{Line5}$=0.6 and $(I_c/I_{pro})_{Line6}$=0.1, the fault current of Line5 was larger than that without both SFCLs. This is attributed to the detour of fault current from Line6 to Line5, where SFCL2 with $(I_c/I_{pro})_{Line6}$=0.1 could effectively limit the fault current in Line6, but SFCL1 with $(I_c/I_{pro})_{Line5}$=0.6 could not limit the fault current in Line5. Such an imbalance operation of SFCL can be understood by the resistance and temperature rise waveforms of SFCL2 on Line6, as shown in Figs. 9(a) and (b) , respectively.

As for the transient stability of power system in Fig. 8(b), the amplitude $\Delta\delta$ of internal phase angle oscillation of G1 in the case of I_c/I_{pro} =0.1 for both SFCLs was smallest and suppressed to 20 % of that without both SFCLs. The similar waveforms have been obtained for the current of Line6, the resistance and temperature rise of SFCL1 and the phase angle of G2, respectively.

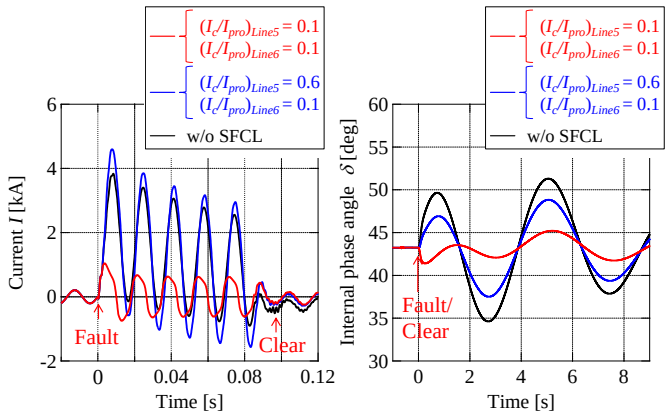

(a) Current of Line5 (b) Internal phase angle of G1

Fig. 8. Current and internal phase angle waveforms

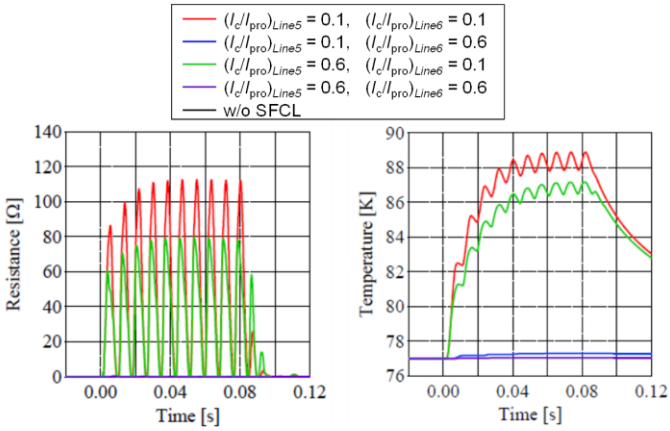

(a) Resistance of SFCL2 (b) Temperature rise of SFCL2

Fig. 9. Resistance and temperature rise waveforms

B. *Fault current limitation coordination*

The coupled analyses in the previous sub-section can give us a strategy for the optimization of operation parameters of SFCLs, i.e. I_c/I_{pro} and I_{op}/I_c on each line, in terms of fault current limitation coordination, which is expected to be reflected to the design and operation of SFCLs.

Here, we assumed the operational criteria of SFCLs as follows:

Fault current limitation: $I_{1st}/I_{pro} < 0.6$
Suppression of internal phase angle oscillation:
$\Delta\delta_{w/SFCL}/\Delta\delta_{w/o\ SFCL} < 0.6$
Load factor in steady state: $I_{op}/I_c < 0.5$

Fig. 10(a) shows the result in the case of Fig. 7, i.e. fault at SS5, SFCL1 on Line 5 and SFCL2 on Line6. The horizontal and vertical axes designate I_c/I_{pro} on Line5 and Line6, respectively, with the corresponding values of I_{op}/I_c. Each criterion is expressed by the dotted line with arrow. In Fig. 10(a), there exists a hatched region to satisfy all criteria, which can be regarded as the optimized parameters of SFCL1 on Line 5 and SFCL2 on Line 6 in the case of fault at SS5.

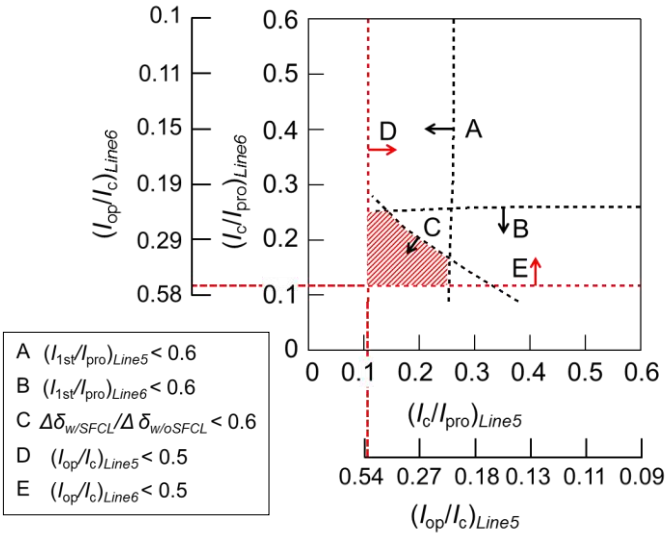

(a) Fault at SS5 with SFCLs on Line5 and Line6 of 77 kV system

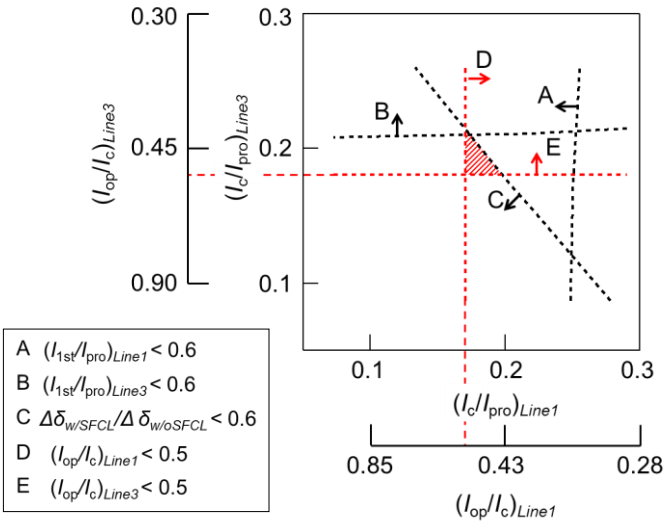

(b) Fault at SS3 with SFCLs on Line1 and Line3 of 275 kV system

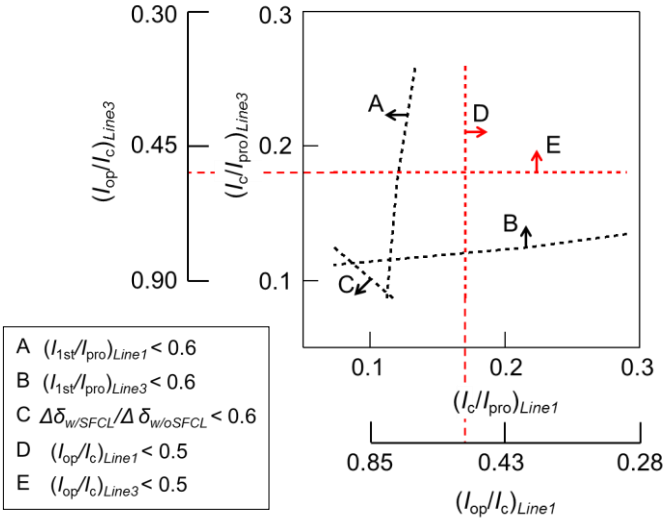

(c) Fault at SS5 with SFCLs on Line1 and Line3 of 275 kV system

Fig. 10. Operation parameters of SFCL based on fault current limitation coordination

Fig. 10(b) shows another result in the case of fault at SS3, SFCL1 on Line1 and SFCL2 on Line3, i.e. in the 275 kV transmission system. There also exists the hatched region, but the area was reduced. Also, Fig. 10(c) shows the result in the case of fault at SS5, SFCL1 on Line1 and SFCL2 on Line3, where the hatched region does not exist. However, in this case, the hatched region can be created by introducing SFCLs not only on Line1 and Line3, but also on Line5 and Line6, i.e. all lines coming to the demand area. Such case studies of coupled analyses are possible for different power systems and fault points for the optimized parameters and introduction points of SFCLs in terms of fault current limitation coordination.

IV. Conclusion

This paper described the fault current limitation coordination in an electric power grid with multiple SFCLs. Coupled analyses of both fault current limitation and transient stability were carried out with PSCAD/EMTDC in a 275/77 kV transmission system model. Simulation results suggested that the operation parameters of SFCLs, such as I_c/I_{pro} and I_{op}/I_c on each line, can be coordinated and optimized in the model system, which is expected to be reflected to the design and operation of SFCLs in order to make their most use, e.g. maximize I_{op}/I_c, in terms of the fault current limitation coordination.

References

[1] "Common Characteristics and Emerging Test Techniques for High Temperature Superconducting Power Equipment", CIGRE WG D1.38 Technical Brochure, No.644 (2015)

[2] M.Noe, "New HTS projects in Europe", IEA ExCo Meeting, Milano, Italy, 30.01.2017

[3] C.-H. Bonnard, F. Sirois, C. Lacroix, G. Didier: "Multi-scale model of resistive-type superconducting fault current limiters based on 2G HTS coated conductors", Superconductor Science Technology, Vol.30, 014005, 2017

[4] H.Kojima, T.Osawa, N.Hayakawa: "Fault Current Limitation Coordination in Power Transmission System with Superconducting Fault Current Limiting Cables (SFCLC)", IEEE Trans. on Applied Superconductivity, Vol.25, Issue 3, Part 2, 5401904 (2015)

[5] W.Paul, M.Chen, M.Lakner, J.Rhyner, D.Braun, W.Lanz: "Fault current limiter based on high temperature superconductors-different concepts, test results, simulations, applications", Physica C, Vol.354, pp.27-33 (2001)

[6] H.Kojima, T.Osawa, N.Hayakawa , M.Hanai, H.Okubo: "Influence of longitudinal temperature distribution on current limiting function of Superconducting Fault Current Limiting Cable (SFCLC)", Journal of Physics: Conference Series (JPCS), Vol.507, No.032026 (2014)

[7] H.Kojima, K.Fukaya, N.Hayakawa, M.Hanai, H.Okubo: "Power Flow Control and Maintenance Strategy of Transformers in Transmission and Distribution Systems", Trans. of IEE Japan, Vol.135-B, No.5, pp.316-321 (2015)